THE JOURNAL OF PHYSICAL CHEMISTRY B

B: Liquids, Chemical and Dynamical Processes in Solution, Spectroscopy in Solution

Dual-Self-Restricted GFP Chromophore Analogues with Significantly Enhanced Emission

Hongping Deng, Chunyang Yu, Deyue Yan, and Xinyuan Zhu

J. Phys. Chem. B, **Just Accepted Manuscript** • DOI: 10.1021/acs.jpcb.9b11329 • Publication Date (Web): 13 Jan 2020

is published by the American Chemical Society. 1155 Sixteenth Street N.W., Washington, DC 20036

Dual-Self-Restricted GFP Chromophore Analogues with Significantly Enhanced Emission

Hongping Deng, Chunyang Yu, Deyue Yan,* and Xinyuan Zhu**

School of Chemistry and Chemical Engineering, State Key Laboratory of Metal Matrix Composites, Shanghai Jiao Tong University, 800 Dongchuan Road, Shanghai 200240, P. R. China. Fax: +86-21-54741297.

To whom correspondence should be addressed:

C.Y. - chunyangyu@sjtu.edu.cn

D.Y. - dyyan@sjtu.edu.cn

X.Z. - xyzhu@sjtu.edu.cn

ABSTRACT

The tremendous gap of fluorescence emission of synthetic green fluorescent protein (GFP) chromophore to the protein itself makes it impossible for applications in molecular and cellular imaging. Here, we developed an efficient methodology to enhance the photoluminescence response of synthetic GFP chromophore analogues by constructing dual-self-restricted chromophores. Single self-restricted chromophores were firstly generated with 2,5-dimethoxy substitution on the aromatic ring, which were further modified with phenyl or 2,5-dimethoxy phenyl to form dual-self-restricted chromophores. This two chromophores showed obvious solvatofluorochromic color palette across blue to yellow with maximum emission Stokes shift of 95 nm, and dramatically enhanced fluorescence emission in various aprotic solvents, especially in hexane, where the QY reached around 0.6. Importantly, in acetonitrile and dimethyl sulfoxide, the fluorescence QYs of both chromophores were over 0.22, which were the highest reported so far in high polar organic solvents. Meanwhile, the fluorescence lifetimes also improved obviously with the maximum of around 4.5 ns. Theoretical calculations revealed a more favorable Mülliken atomic charge translocation over the double-bond bridge and illustrated much higher energy barriers for the Z/E photoisomerization together with larger bond orders compared to the GFP core chromophore, *p*-HBDI. Our work significantly improved the fluorescence emission of synthetic GFP chromophore analogues in polar solvents while reserved the multicolor emitting function, providing a solid molecular motif for engineering high-performance fluorescent probes.

KEYWORDS: Fluorescent dyes, aggregation-induced emission, fluorescent proteins, green fluorescent protein chromophore, photoisomerization.

INTRODUCTION

The genetically encoded green fluorescent protein (GFP) has provided a powerful tool for labeling and tracing biological targets in biochemistry and cell biology.[1-4] The discovery and development of fluorescent family have achieved simultaneous multicolor imaging of a variety of biomolecules, and deep tissue or live animal imaging with red to near-infrared proteins.[5-9] However, the fluorescence quantum yields (QYs) dropped dramatically over four orders of magnitude for denatured proteins.[10] It is beneficial to understand protein photophysics, develop new fluorescent probes and find potential applications by investigating chemically synthesized GFP chromophore and its analogues.[11,12] The loss of fluorescence for these chromophores significantly hindered this process, owing to an ultrafast internal conversion due to free molecular motions of the carbon-carbon bonds.[13-17]

A variety of methodologies have been applied to increase the QYs of these chromophores by inhibiting the nonradiative pathways over past years.[18,19] Physical encapsulation with different hosts, such as proteins,[20,21] ribonucleic acids,[22,23] amphiphilic macromolecules,[24] porous scaffolds,[25] has greatly improved the corresponding fluorescence response, but significantly increased the overall probe size, making it difficult for further molecular labeling. Chemical locking with covalent bonds or metal chelation,[26-29] results in very high fluorescence QYs comparable to commercial dyes, but loses multicolor emitting function, which is important for constructing responsive probes. Similar loss of multicolor emission happens for hydrogen-bond locking chromophores, which generally shows low QYs in different fluid solvents.[30,31]

Meanwhile, although tremendous efforts have been made to make highly emissive unlocked GFP chromophore analogues, there is very limited progress in enhancing the emission, especially in

high polar solvents.[18,19] The most widely utilized strategy was to increase the molecular conjugation length at the aromatic or azalactone ring, but the efficacy was still limited due to efficient molecular motions.[32-34] Meta-amine GFP-like chromophores were synthesized and reported to have QYs over 0.4 in hexane, but dropped below 0.1 in polar aprotic solvent, acetonitrile.[35] Further modification with a push-pull substituent on the phenyl ring, the QY of the corresponding chromophore increased to 0.6 in hexane, but still was less than 0.1 in acetonitrile.[36] Recently, pyridinium analogues of GFP chromophore were reported to have very good QYs in water, but still very low in polar organic solvents, which might be due to the poor solubility in water.[37] We have disclosed an unusual enhancement of fluorescence emission for 2,5-dialkoxy-substituted GFP-like chromophores with QYs over 0.1 in polar solvents, such as acetonitrile, dimethylformamide and dimethyl sulfoxide, due to the formation of a self-restricted effect.[38] It would be very interesting to investigate the impact of dual-self-restricted effects on the fluorescence response of the chromophores.

Here, we designed and synthesized two dual-self-restricted GFP-like chromophores by the standard Erlenmeyer azalactone methodology. The fluorescence response in various solvents were studied, showing significant emission enhancement in all tested solvents, especial unexpected improvement in high polar solvents. Theoretical calculations further revealed the molecular mechanism due to increased rotation energy barrier along the carbon-carbon double bond.

RESULTS AND DISCUSSION

Synthetic GFP-like chromophores are non-emissive owing to the ultrafast internal conversion along the carbon-carbon bonds.[13-15] Theoretically, an efficient methodology to inhibit the carbon-carbon molecular motions would adopt locking strategy at both the aromatic and azalactone rings. Thus, single non-covalent "locking" with self-restricted effect was designed at the aromatic ring, while a second restriction was applied to the azalactone ring via phenyl or 2,5-dimethoxy-phenyl substitution, resulting in dual-self-restricted chromophores (**Scheme 1a**). Considering the synthetic liability and chemical reactivity, these two compounds, 4-(2,5-methoxybenzylidene)-2-phenyloxazol-5(4H)-one (MBDPO) and 4-(2,5-methoxybenzylidene)-2-(2,5-methoxyphenyloxazol)-5(4H)-one (MBDMPO), were prepared into oxazolone analogues via the standard Erlenmeyer synthesis[39,40] with relatively good yields, which included the cyclization reaction between benzaldehyde and benzoylglycine derivatives. For MBDMPO, the benzoylglycine derivative was prepared via a two-step process, which contained an amidation reaction between 2,5-dimethoxybenzoic acid and glycine methyl ester hydrochloride, and a hydrolysis reaction of the corresponding ester product. The synthetic procedure was given in **Scheme 1b** and the molecular structures of the two chromophores were shown together with that of GFP core chromophore, *p*-HBDI. The chemical structures of MBDPO and MBDMPO were fully characterized, and detailed synthetic procedures and characterizations were provided in the Supporting Information.

The optical properties of the two chromophores were firstly tested in ethyl acetate (EA, a good solvent). As shown in **Figure 1**, the absorption spectra of MBDMPO and MBDPO displayed two major peaks at around 340 nm and 425 nm respectively ascribing to electron transitions from π-π* and n-π*.[41] The substitution with 2,5-dimethoy group for MBDMPO weakened the electron

transition from π-π*, but strengthened that from n-π*, making the second absorption peak red-shifted compared to that of MBDPO. Generally, GFP-like chromophores are very dim in fluid solvents due to free rotation along either the single or double bond, resulting in significant fluorescence quenching.[18,19] On the contrary, the inhibition of either the single or double bond would lead to the increase of fluorescence emission. For the two chromophores, an important question was whether they could display obvious fluorescence in fluid solvent at room temperature. Apparently, bright green fluorescence was observed for both MBDMPO and MBDPO in EA with emission peaks at 509 nm and 516 nm, respectively. These emission peaks red-shifted more than 80 nm compared to that of *p*-HBDI due to self-restricted effect and increased conjugation at the heterocyclic ring. Moreover, the fluorescence quantum yields and lifetimes of MBDMPO and MBDPO were also tested in EA to determine the degree of fluorescence emission enhancement (**Table S1, Table S2**). The QYs of MBDMPO and MBDPO were about 0.36 and 0.34 with fluorescence lifetimes of around 3.1 ns and 3.9 ns, respectively, which improved significantly compared to the core chromophore (*p*-HBDI) and other unlocked GFPc analogs,[18,19] suggesting the effective inhibition of carbon-carbon molecular motions.

To prove the generosity of the enhanced emission, the solvent dependence of fluorescence emission for MBDMPO and MBDPO was further investigated in different solvents. As given in **Figure 2**, the absorption spectra for both chromophores showed minor changes with increasing solvent polarity from Hex to MeOH,[42] displaying obvious two-peak absorptions for π-π* and n-π* transition. One feature was the redshift of the absorption for n-π* transition along with increasing polarity, which was still less than 15 nm in all solvents tested. The other feature was the enhanced absorption intensity for π-π* transition compared to that of n-π* transition in MeOH owing to the formation of strong solvent-solute hydrogen bonding.[35,43] Meanwhile, intense fluorescence

emission could be observed from hexane (Hex) to methanol (MeOH) for both MBDPO and MBDMPO, proving the existence of the emission enhancement for the two chromophores. Specifically, the emission spectra of MBDMPO had only one emission peak, which further redshifted from 478 nm to 552 nm with distensible half band width from Hex to MeOH, displaying obvious solvatofluorochromism feature.[35-37] Meanwhile, the fluorescence QYs and lifetimes of MBDMPO in these solvents were also tested to tell the degree of emission enhancement. In Hex, the QY of MBDMPO reached around 0.6, which was unexpectedly high for unlocked GFP-like chromophores.[18,19] With the increase of solvent polarity, the emission QY decreased to 0.28 in DMSO and further decreased to 0.05 in MeOH due to strong solvent-solute hydrogen-bonding effect.[35,43] The solvent-solute H-bonding effect was proposed by previously published literatures,[14,35] where the H-bond donor (methanol) and the imidazolinone group formed a type of H-bonded intermediate, inducing a new nonradiative decay channel responsible for fluorescence loss. The predominant H-bonded intermediate was through solvent hydrogen binding to the carbonyl oxygen, other than the nitrogen of the imidazolinone group. The lifetimes of MBDMPO were at about 2.4 ns to 3.2 ns from Hex to DMSO, but also decreased to 0.9 ns in MeOH (**Table S1, Figure S1**). Likely, the solvent dependence of MBDPO followed the same phenomenon as that of MBDMPO. From Hex to MeOH, the emission peak of MBDPO also redshifted to 555 nm with a maximum Stokes shift of about 93 nm. The emission response of MBDPO was greatly enhanced with fluorescence QYs between 0.41 and 0.22, and lifetimes between 2.6 ns and 4.5 ns from Hex to DMSO, which decreased to 0.06 and 1.8 ns in MeOH (**Table S2, Figure S2**). Importantly, the fluorescence QYs of both chromophores were over 0.22 in high polar solvents, acetonitrile and dimethyl sulfoxide, which were the highest reported for unlocked GFP-like chromophores to our knowledge in polar organic solvents. In short, the fluorescence performance

of these two chromophores enhanced greatly in a variety of solvents, reflecting efficient inhibition of carbon-carbon bond molecular motions.

To investigate the influence of solvent-solute hydrogen bonding on fluorescence quenching, the titration of MBDMPO and MBDPO in acetonitrile (ACN) with methanol was conducted with increasing amount of hydrogen donor. As shown in **Figure 3**, for both chromophores, the fluorescence intensity decreased gradually with the increasing content of MeOH in ACN from 0 to 250 μL, demonstrating the fluorescence quenching effect due to strong solvent-solute hydrogen bonding.[35,36] At the same time, the decrease of emission intensity for MBDMPO was much greater than that of MBDPO, which proved that the solvent-solute hydrogen bonding was stronger for MBDMPO. Fitting hydrogen donor amount (volume) with emission intensity, the fluorescence quenching followed into an exponential decay manner for both chromophores. Meanwhile, the effect of deuterated solvent on the fluorescence emission of MBDMPO and MBDPO was also measured. The addition of MeOD in MeOH increased the emission intensity for both chromophores, which further revealed the fluorescence quenching of hydrogen bonding.[38] And, the emission enhancement for MBDMPO was more significant than that of MBDPO under the same condition, which also illustrated the stronger solvent-solute hydrogen bonding for MBDMPO compared to MBDPO.

A phenomenon induced by restriction of intramolecular rotation (RIR) was defined as aggregation-induced emission (AIE), where the typical carbon-carbon single bond molecular motions were greatly inhibited in aggregated state.[44,45] It is interesting to see if these two chromophores could have strong emission in both fluid solvents and aggregated state. Since both chromophores have bright fluorescence in fluid solvents, the linear-relationship between chromophore concentration and fluorescence emission was measured to make sure there was no aggregation due to high

concentration of chromophores.[46] **Figure S3** proved that there was a good linear relationship for MBDPO and MBDMPO between chromophore concentration and emission intensity when the concentration was less than 10 μM in acetonitrile (a good solvent). A MeOH/water mixed solvent system was selected to explore the emission response in aggregated state because the QYs of both chromophores were the lowest in methanol among tested solvents. In the cases of AIE fluorophores, the emission intensity would increase slowly until exceeding a certain amount of bad solvent (usually water) in the mixed solvent.[44] As shown in **Figure 4**, the fluorescence intensity decreased hugely under 50% water content in the mixed solvents for both chromophores, which most likely was due to solvatochromic effect. Under higher water content, the emission intensity recovered and enhanced to a maximum of about 2.3-fold increase compared to that in MeOH, but it was still not able to compete with QYs in aprotic solvents. The enhanced emission was ascribed to aggregation-induced emission,[44,45] where the formation of molecular aggregates greatly inhibited the free molecular motions of the corresponding chromophores, leading to the increment of emission intensity. Meanwhile, there was a general redshift phenomena of the emission peaks with a maximum Stokes shift of about 20 nm, which might be due to solvent-solute interaction or chromophore aggregation.[35,47] Under 90% water content, the emission intensity decreased for MBDMPO but increased for MBDPO with similar molecular structure. The introduction of two methoxy groups decreased the overall coplanar conformation for MBDMPO, leading to the formation of less ordered aggregates under higher water content.[47] Together, these results might suggest that the dual-self-restricted strategy might be able to produce highly emissive GFP-like chromophores in both solutions and aggregates with molecular tailoring.

To reveal the mechanism for improved fluorescence response, theoretical calculations were employed to compare the difference of the three chromophores (**Scheme 1a**). The optimum

geometries of *p*-HBDI, MBDMPO and MBDPO molecules calculated from density functional theory (DFT) calculations (in gas phase) are provided in **Figure 5**.[48] We can find along with the rotation around the double bond between the imidazolinone heterocycle and the aromatic ring, *p*-HBDI and MBDPO have two configurations, while MBDMPO has four configurations. In the meanwhile, the relative energies of the most stable structures for these molecules are also calculated. Specifically, *p*-HBDI 2 relative to *p*-HBDI 1 is 2.70 kcal/mol; MBDPO 2 relative to MBDPO 1 is 3.50 kcal/mol; MBDMPO A2 relative to MBDMPO A1 is 4.13 kcal/mol; MBDMPO B2 relative to MBDMPO B1 is 3.45 kcal/mol. It should be noted that each *Z*-*E* isomerization path corresponds to one radiationless decay channel in the excited state. So, the increment of isomerization barrier in the excited state is beneficial for the improvement of the fluorescence performance.

Also, the electron density distribution for these compounds were further analysed.[49,50] As given in **Figure S4 and S5**, the HOMO of MBDPO is delocalized over the aromatic and the azalactone heterocycle, and the phenyl ring has less contribution. Meanwhile, the HOMO-1, LUMO and LUMO+1 are delocalized over the whole molecule, which means the electron will transfer along the double bond between the aromatic and the azalactone heterocycle upon excitation. In contrast, the HOMO-1 of MBDMPO is localized over the two phenyl rings and the azalactone heterocycle has less contribution. The HOMO, LUMO and LUMO+1 are the out-of-phase and in-phase combination of three localized π bonds, and all of them are delocalized over the whole molecule. However, we can find that the introduction of methoxy group increases the conjugation of molecule MBDMPO. Thus, relative to molecule MBDPO, a red shift of n-π* absorption for MBDMPO has been observed both in experiments and theoretical calculations (**Figure S6**). Moreover, the obvious solvatofluorochromism feature is observed for all the optimized structures

of both MBDPO and MBDMPO (**Figure S7**), which is also in accordance with experimental results.

Meanwhile, previous works have shown that the translocation of the negative charge from the aromatic ring to the azalactone heterocycle favours to restrict the motion around the exocyclic double bond and inhibit this radiationless channel.[38,51,52] As shown in **Figure 6**, the negative charges are mainly located on aromatic ring for MBDMPO and MBDPO molecule at S0 state, and then it has an obviously charge translocation from aromatic ring to azalactone heterocycle upon excitation, which will be favorable to inhibit the radiationless decay channel around the exocyclic double bond. Meanwhile, the charge transfer (S1-S0) for heterocycle upon excitation is very similar for three chromophores, but there is a major difference for the aromatic ring (**Table S3**). The aromatic ring charge transfer (S1-S0) order for the three chromophores is MBDMPO > MBDPO > *p*-HBDI, which means a bigger part of charge is transferred to the double bond with the same order as MBDMPO > MBDPO > *p*-HBDI. The more electrons transfer to the double bond bridge, the better Z/E photoisomerization inhibition. Thus, the calculated results are agreed well with the experimental data that the fluorescence emission response follows the order as MBDMPO > MBDPO > > *p*-HBDI.

Moreover, the stability of the twisted state relative to the *Z*-isomer state for *p*-HBDI, MBDPO and MBDMPO has been examined by time-dependent density function theory (TDDFT) calculations.[14,36,53] As shown in **Figure 7a**, the size of the stability of twisted state is in the order of *p*-HBDI (-6.40 kcal/mol) > MBDMPO A (7.13 kcal/mol) > MBDMPO B (7.74 kcal/mol) > MBDPO (8.30 kcal/mol). Although the order of the relative stability of twisted state is not the same as the order of the fluorescence performance, the higher relative energy for MBDPO and MBDMPO than *p*-HBDI indeed support its fluorescence enhancement. The substituent electronic

effect on the isomerization process is more complicated than the relative energies of the *Z*-isomer and twisted states.[36] To further have a comparison between MBDPO and MBDMPO, a Mayer bond analysis was performed.[54-56] As shown in **Figure 7b**, the C=C bond order of MBDPO 1 and MBDMPO A1 are 1.8120 and 1.9578, respectively, which is much higher than *p*-HBDI (1.5840). As we know, the higher bond order is closely related to the higher rotation energy barriers. That is to say, the introduction of the methoxy group further increases the conjugation of C=C bond in molecule MBDMPO. Consequently, molecule MBDMPO has a relatively better fluorescence performance than molecule MBDPO.

CONCLUSION

It is a big puzzle that synthetic GFP-like chromophores generally are non-emissive in solution while remain their excellent optical properties in intact proteins.[4-6,18] In this work, we have developed emission significantly enhanced dual-self-restricted chromophores, which were highly emissive in polar solvents and showed variable emission color palette from blue to yellow due to the self-restricted effect and conjugated effect. Moreover, the mechanism for the enhanced emission response was illustrated via theoretical calculations of the Mülliken atomic charge translocation, the rotation energy barrier and the Mayer bond order, showing increased energy barriers for Z/E photoisomerization. The dual-self-restricted chromophores were designed to be functionalizable at multiple positions via different chemical synthesis approaches. With enhanced fluorescence response of variable emission color palette, these chromophores are suitable for the development of functional fluorescent probes for molecular and cellular applications.

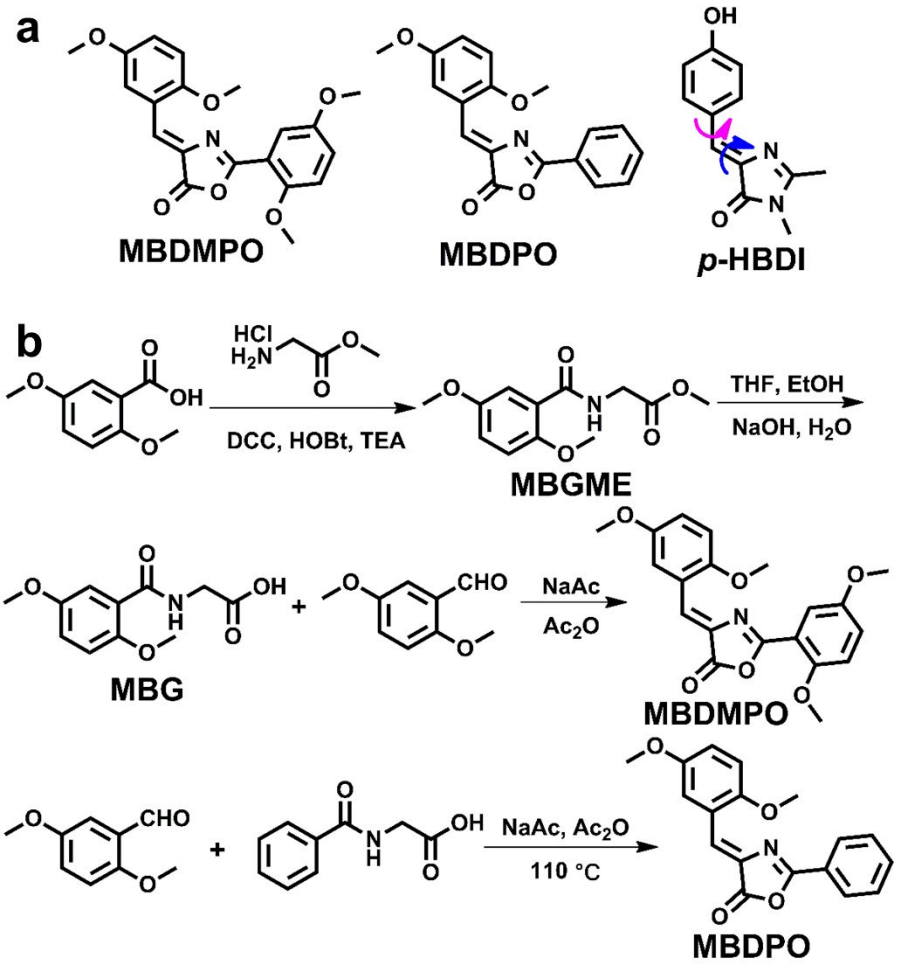

Scheme 1. Design and synthesis of two dual-self-restricted GFP-like chromophores. **(a)** Molecular structures of the two chromophores with the GFP core chromophore, p-HBDI, showing efficient molecular motions along the carbon-carbon bonds. **(b)** Synthetic routes towards the dual-self-restricted chromophores, MBDMPO and MBDPO, via the standard Erlenmeyer synthesis.

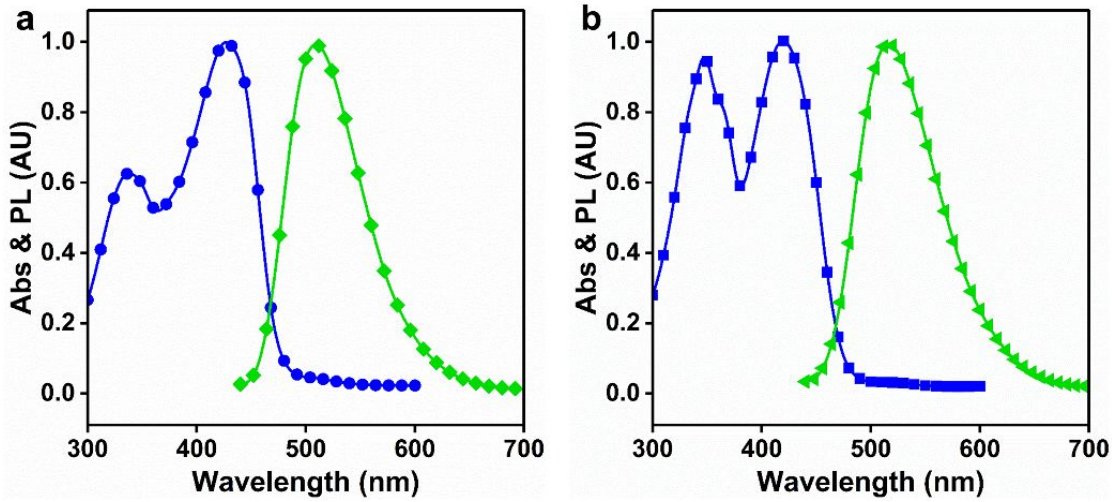

Figure 1. The optical properties of the two chromophores in good solvent, ethyl acetate (EA). Normalized absorption (blue) and fluorescence emission (green) spectra of MBDMPO **(a)** and MBDPO **(b)** in EA. Both chromophores showed enhanced bright green fluorescence. Emission spectra were excited at maximum of absorption.

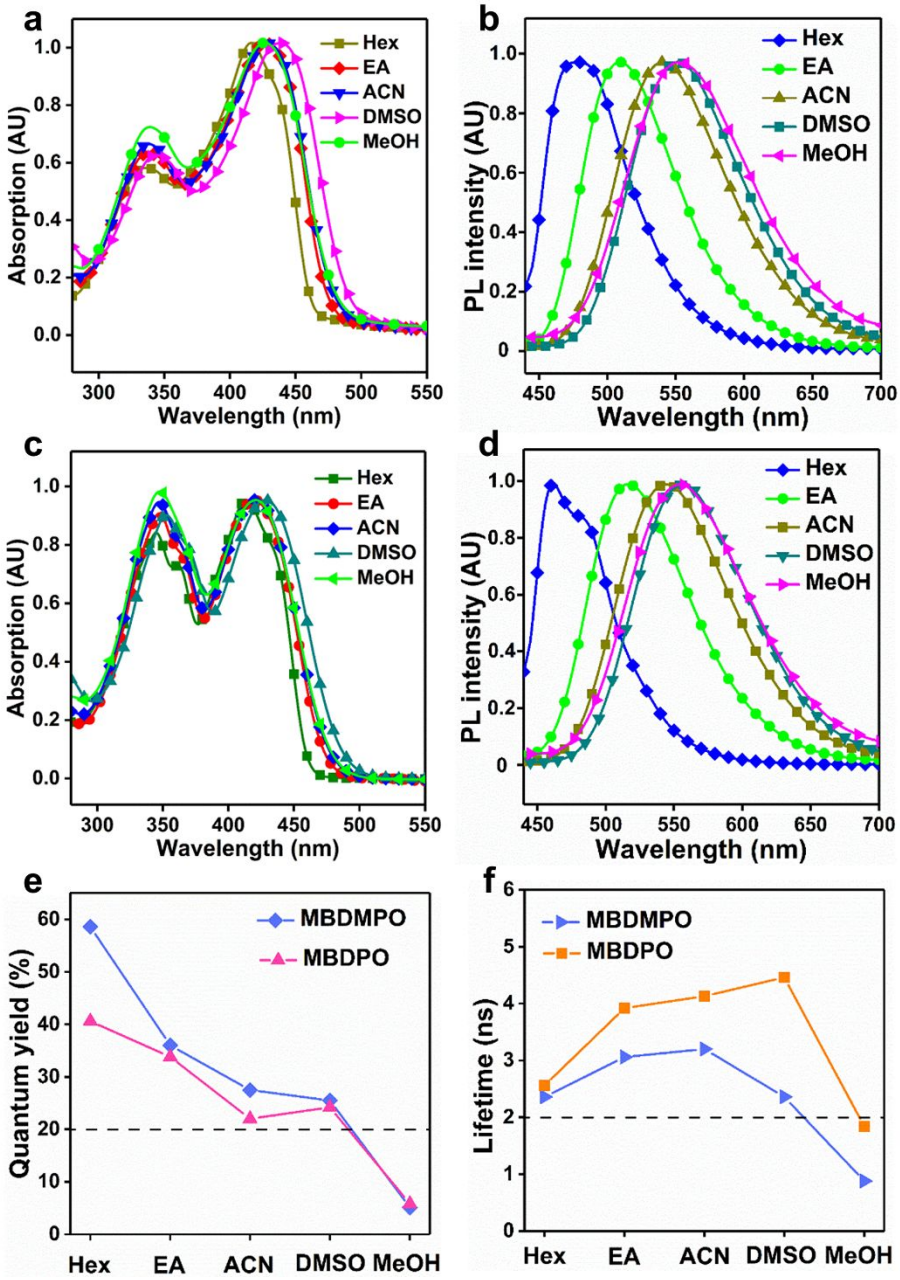

Figure 2. The effect of solvent polarity on the optical properties of the two chromophores. Normalized absorption **(a, c)** and fluorescence emission **(b, d)** spectra of MBDMPO **(a, b)** and MBDPO **(c, d)** in different solvents. The fluorescence quantum yield **(e)** and lifetime **(f)** of MBDMPO and MBDPO in different solvents, showing significantly increased QYs, especially in high polar solvents. The emission spectra were excited using the maximum absorption.

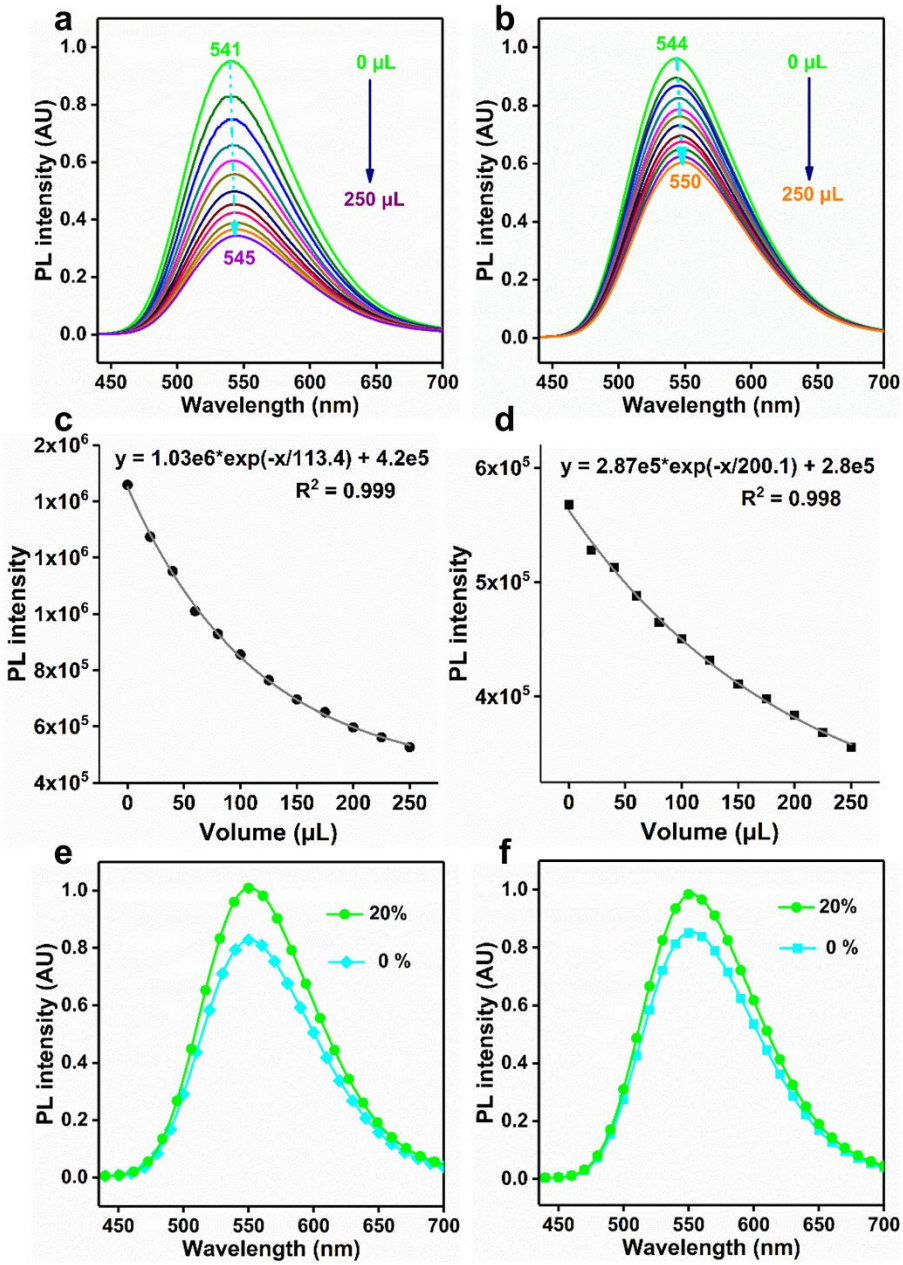

Figure 3. The effect of solvent-solute hydrogen bonding on the optical properties of the two chromophores. The fluorescence emission of MBDMPO **(a)** and MBDPO **(b)** in acetonitrile with increasing methanol (MeOH) from 0 μL to 250 μL. The exponential fitting of emission intensity to methanol volume for MBDMPO **(c)** and MBDPO **(d)** with equations and R^2 values. The normalized fluorescence emission of MBDMPO **(e)** and MBDPO **(f)** in MeOH/MeOD mixed solvents. The ratio of MeOD in MeOH was given.

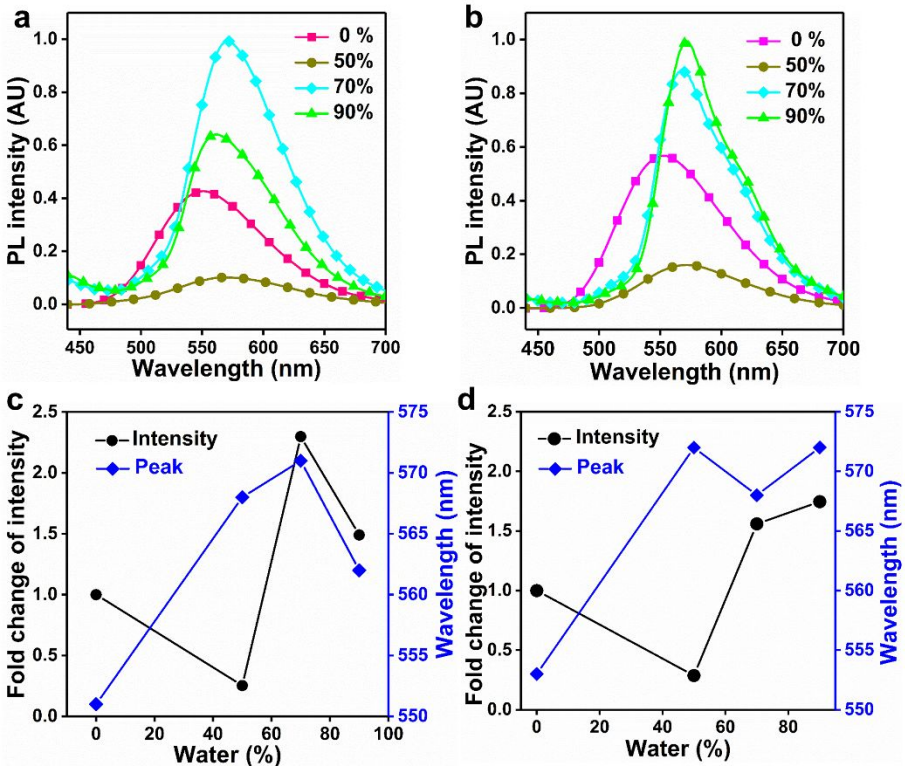

Figure 4. The effect of aggregation on the optical properties of the two chromophores. The fluorescence emission **(a, b)** and its fold change of fluorescence intensity together with the change of emission peak **(c, d)** for MBDMPO **(a, c)** and MBDPO **(b, d)** in mixed solvents of MeOH/H_2O with increasing water content in percentage. The emission spectra were excited using the maximum absorption wavelengths in methanol.

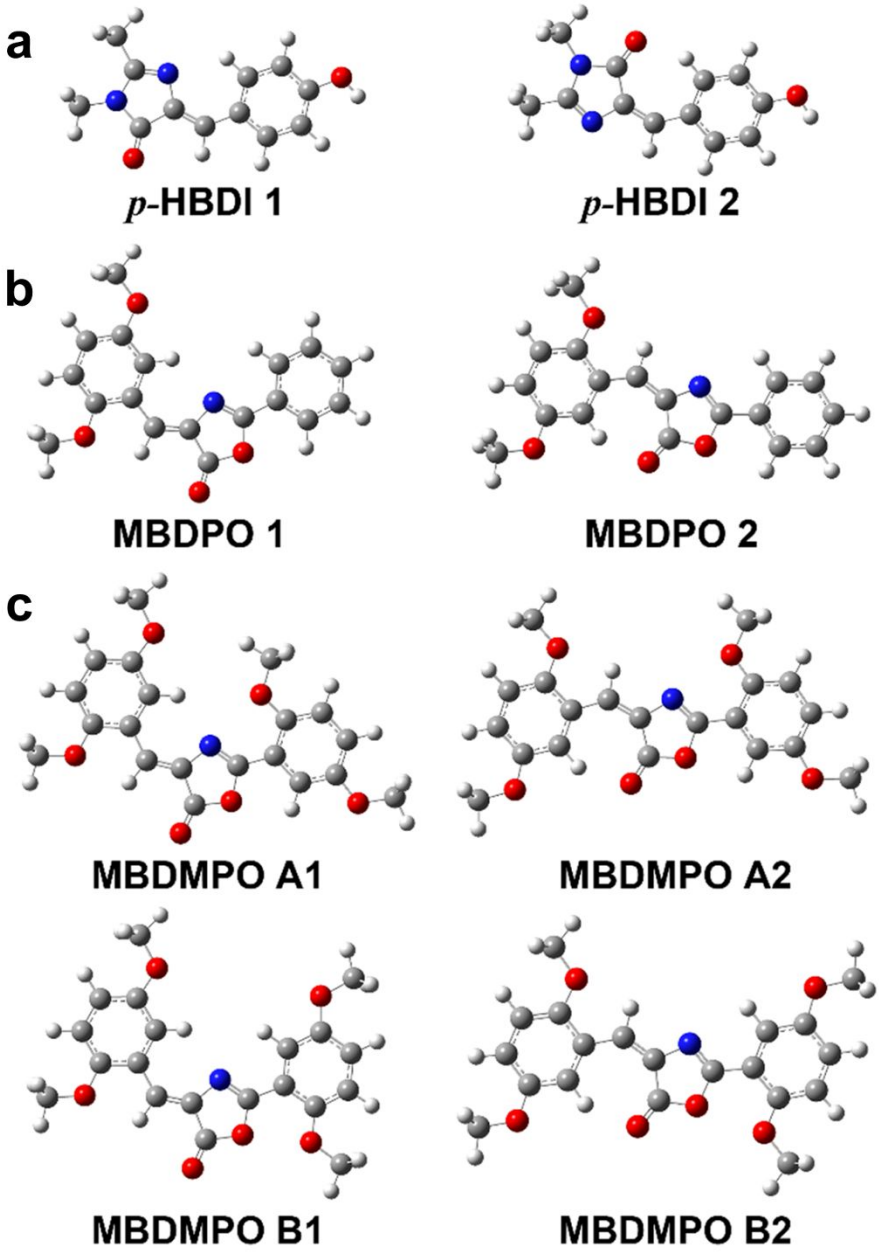

Figure 5. The optimized structures of three chromophores in gas phase obtained from DFT calculations to obtain the most stable configuration of each chromophore. Different molecular configurations for *p*-HBDI **(a)**, MBDMPO **(b)** and MBDPO **(c)** with Z-configuration **(1)** or *E*-configuration **(2)** were presented, while MBDMPO showed four configurations.

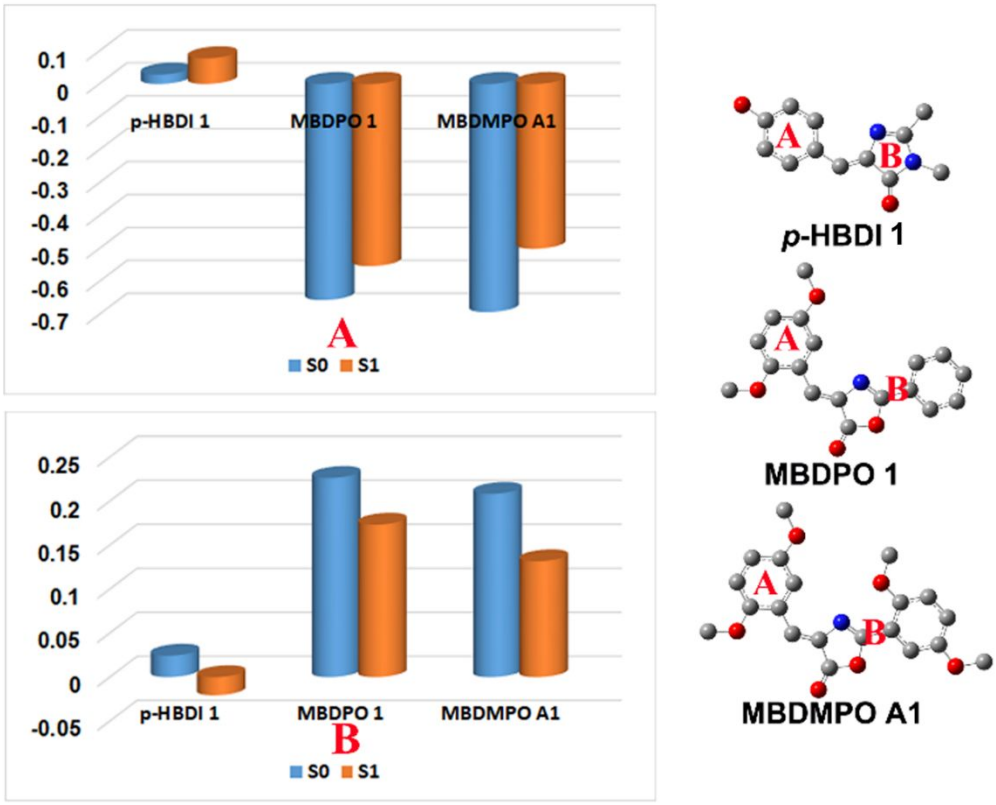

Figure 6. The Mülliken atomic charge variation of aromatic ring **(A)** and imidazolinone heterocycle **(B)** upon excitation (S0-S1) for *p*-HBDI 1, MBDPO 1 and MBDMPO A1 from DFT calculations. Chromophores with the most stable configuration were selected to calculate the charge transfer. The atomic charge of the bridge carbon is not included in the sum.

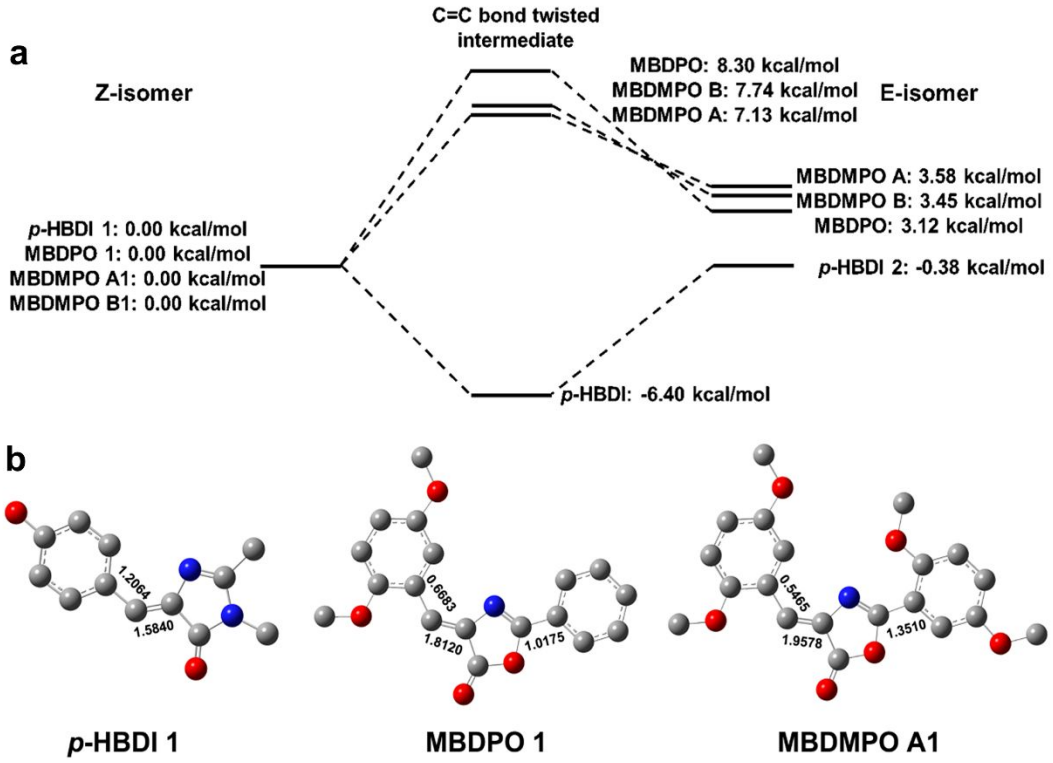

Figure 7. Theoretical simulations revealed much higher Z/E photoisomerization barriers of the two chromophores. **(a)** The TDDFT calculated relative energies (kcal/mol) of the Z* (the reference state), the twisted intermediate, and E* states of MBDMPO, MBDPO and *p*-HBDI. **(b)** The Mayer bond order analysis of molecule MBDMPO A1, MBDPO 1 and *p*-HBDI from DFT calculations.

ASSOCIATED CONTENT

Supporting Information. Synthesis, characterizations, time-resolved fluorescence and emission spectra (Figure S1 to Figure S3), optical parameters (Table S1, Table S2) and theoretical calculations data (Figure S4 to Figure S7, Table S3).

AUTHOR INFORMATION

Corresponding Authors

*E-mail: chunyangyu@sjtu.edu.cn (C.Y.).

*E-mail: dyyan@sjtu.edu.cn (D.Y.)

*E-mail: xyzhu@sjtu.edu.cn (X.Z.).

Notes

The authors declare no competing financial interests.

ACKNOWLEDGMENT

We acknowledge financial support from the National Basic Research Program of China (2015CB931801) and the National Natural Science Foundation of China (51473093, 21404070).

ABBREVIATIONS

Hex: *n*-hexane; EA: ethyl acetate; ACN: acetonitrile; DMSO: dimethyl sulfoxide; MeOH: methanol.

REFERENCES

1. Tsien, R. Y. The Green Fluorescent Protein. *Annu. Rev. Biochem.* **1998**, *67*, 509-544.

2. Chalfie, M.; Tu, Y.; Euskirchen, G.; Ward, W. W.; Prasher, D. C. Green Fluorescent Protein as a Marker for Gene Expression. *Science* **1994**, *263*, 802-805.

3. Misteli, T.; Spector, D. L. Applications of the Green Fluorescent Protein in Cell Biology and Biotechnology. *Nat. Biotechnol.* **1997**, *15*, 961-964.

4. Tsien, R. Y. Constructing and Exploiting the Fluorescent Protein Paintbox. *Angew. Chem. Int. Ed.* **2009**, *48*, 5612-5626.

5. Hoffman, R. M. The Multiple Uses of Fluorescent Proteins to Visualize Cancer *In Vivo*. *Nat. Rev. Cancer* **2005**, *5*, 796-806.

6. Giepmans, B. N. G.; Adams, S. R.; Ellisman, M. H.; Tsien, R. Y. The Fluorescent Toolbox for Assessing Protein Location and Function. *Science* **2006**, *312*, 217-224.

7. Kremers, G.-J.; Gilbert, S. G.; Cranfill, P. J.; Davidson, M. W.; Piston, D. W. Fluorescent Proteins at a Glance. *J. Cell Sci.* **2011**, *124*, 157-160.

8. Shcherbakova, D. M.; Verkhusha, V. V. Near-Infrared Fluorescent Proteins for Multicolor *In Vivo* Imaging. *Nat. Methods* **2013**, *10*, 751-754.

9. Fukuyama, S.; Katsura, H.; Zhao, D.; Ozawa, M.; Ando, T.; Shoemaker, J. E.; Ishikawa, I.; Yamada, S.; Neumann, G.; Watanabe, S.; Kitano, H.; Kawaoka, Y. Multi-Spectral Fluorescent Reporter Influenza Viruses (Color-Flu) as Powerful Tools for *In Vivo* Studies. *Nat. Commun.* **2015**, *6*, 6600.

10. Enoki, S.; Saeki, K.; Maki, K.; Kuwajima, K. Acid Denaturation and Refolding of Green Fluorescent Protein. *Biochemistry* **2004**, *43*, 14238-14248.

11. Follenius-Wund, A.; Bourotte, M.; Schmitt, M.; Iyice, F.; Lami, H.; Bourguignon, J. J.; Haiech, J.; Pigault, C. Fluorescent Derivatives of the GFP Chromophore Give a New Insight into the GFP Fluorescence Process. *Biophys. J.* **2004**, *85*, 1839-1850.

12. Pakhomov, A. A.; Martynov, V. I. GFP Family: Structural Insights into Spectral Tuning. *Chem. Biol.* **2008**, *15*, 755-764.

13. Baffour-Awuah, N. Y. A.; Zimmer, M. Hula-Twisting in Green Fluorescent Protein. *Chem. Phys.* **2004**, *303*, 7-11.

14. Yang, J. S.; Huang, G. J.; Liu, Y. H.; Peng, S. M. Photoisomerization of the Green Fluorescence Protein Chromophore and the Meta- and Para-Amino Analogues. *Chem. Commun.* **2008**, 1344-1346.

15. Meech, S. R. Excited State Reactions in Fluorescent Proteins. *Chem. Soc. Rev.* **2009**, *38*, 2922-2934.

16. Baldridge, A.; Samanta, S. R.; Jayaraj, N.; Ramamurthy, V.; Tolbert, L. M. Steric and Electronic Effects in Capsule-Confined Green Fluorescent Protein Chromophores. *J. Am. Chem. Soc.* **2011**, *133*, 712-715.

17. Mooney, C. R. S.; Horke, D. A.; Chatterley, A. S.; Simperler, A.; Fielding, H. H.; Verlet, J. R. R. Taking the Green Fluorescent Out of the Protein: Dynamics of the Isolated GFP Chromophore Anion. *Chem. Sci.* **2013**, *4*, 921-927.

18. Tolbert, L. M.; Baldridge, A.; Kowalik, J.; Solntsev, K. M. Collapse and Recovery of Green Fluorescent Protein Chromophore Emission through Topological Effects. *Acc. Chem. Res.* **2012**, *45*, 171-181.

19. Deng, H.; Zhu, X. Emission Enhancement and Application of Synthetic Green Fluorescent Protein Chromophore Analogs. *Mater. Chem. Front.* **2017**, *1*, 619-629.

20. Baldridge, A.; Feng, S. H.; Chang, Y. T.; Tolbert, L. M. Recapture of GFP Chromophore Fluorescence in a Protein Host. *ACS Comb. Sci.* **2011**, *13*, 214-217.

21. Lee, J. S.; Baldridge, A.; Feng, S.; SiQiang, Y.; Kim, Y. K.; Tolbert, L. M.; Chang, Y. T. Fluorescence Response Profiling for Small Molecule Sensors Utilizing the Green Fluorescent Protein Chromophore and Its Derivatives. *ACS Comb. Sci.* **2011**, *13*, 32-38.

22. Paige, J. S.; Wu, K. Y.; Jaffrey, S. R. RNA Mimics of Green Fluorescent Protein. *Science* **2011**, *333*, 642-646.

23. Paige, J. S.; Nguyen-Duc, T.; Song, W. J.; Jaffrey, S. R. Fluorescence Imaging of Cellular Metabolites with RNA. *Science* **2012**, *335*, 1194.

24. Deng, H. P.; Su, Y.; Hu, M. X.; Jin, X.; He, L.; Pang, Y.; Dong, R. J.; Zhu, X. Y. Multicolor Fluorescent Polymers Inspired from Green Fluorescent Protein. *Macromolecules* **2015**, *48*, 5969-5979.

25. Williams, D. E.; Dolgopolova, E. A.; Pellechia, P. J.; Palukoshka, A.; Wilson, T. J.; Tan, R.; Maier, J. M.; Greytak, A. B.; Smith, M. D.; Krause, J. A.; Shustova, N. B. Mimic of the Green

Fluorescent Protein β-Barrel: Photophysics and Dynamics of Confined Chromophores Defined by a Rigid Porous Scaffold. *J. Am. Chem. Soc.* **2015**, *137*, 2223-2226.

26. Wu, L. X.; Burgess, K. Syntheses of Highly Fluorescent GFP Chromophore Analogues. *J. Am. Chem. Soc.* **2008**, *130*, 4089-4096.

27. Baranov, M. S.; Lukyanov, K. A.; Borissova, A. O.; Shamir, J.; Kosenkov, D.; Slipchenko, L. V.; Tolbert, L. M.; Yampolsky, I. V.; Solntsev, K. M. Conformationally Locked Chromophores as Models of Excited-State Proton Transfer in Fluorescent Proteins. *J. Am. Chem. Soc.* **2012**, *134*, 6025-6032.

28. Hsu, Y. H.; Chen, Y. A.; Tseng, H. W.; Zhang, Z. Y.; Shen, J. Y.; Chuang, W. T.; Lin, T. C.; Lee, C. S.; Hung, W. Y.; Hong, B. C.; Liu, S. H.; Chou, P. T. Locked Ortho- and Para-Core Chromophores of Green Fluorescent Protein; Dramatic Emission Enhancement *via* Structural Constraint. *J. Am. Chem. Soc.* **2014**, *136*, 11805-11812.

29. Baldridge, A.; Solntsev, K. M.; Song, C.; Tanioka, T.; Kowalik, J.; Hardcastle, K.; Tolbert, L. M. Inhibition of Twisting of a Green Fluorescent Protein-Like Chromophore by Metal Complexation. *Chem. Commun.* **2010**, *46*, 5686-5688.

30. Chen, K.-Y.; Cheng, Y.-M.; Lai, C.-H.; Hsu, C.-C.; Ho, M.-L.; Lee, G.-H.; Chou, P.-T. Ortho Green Fluorescence Protein Synthetic Chromophore; Excited-State Intramolecular Proton Transfer *via* a Seven-Membered-Ring Hydrogen-Bonding System. *J. Am. Chem. Soc.* **2007**, *129*, 4534-4535.

31. Chuang, W. T.; Hsieh, C. C.; Lai, C. H.; Lai, C. H.; Shih, C. W.; Chen, K. Y.; Hung, W. Y.; Hsu, Y. H.; Chou, P. T. Excited-State Intramolecular Proton Transfer Molecules Bearing o-

Hydroxy Analogues of Green Fluorescent Protein Chromophore. *J. Org. Chem.* **2011**, *76*, 8189-8202.

32. He, X.; Bell, A. F.; Tonge, P. J. Synthesis and Spectroscopic Studies of Model Red Fluorescent Protein Chromophores. *Org. Lett.* **2002**, *4*, 1523-1526.

33. Huang, G. J.; Yang, J. S. The *N*-Arylamino Conjugation Effect in the Photochemistry of Fluorescent Protein Chromophores and Aminostilbenes. *Chem. Asian J.* **2010**, *5*, 2075-2085.

34. Huang, G.; Zhang, G.; Wu, Y.; Liao, Q.; Fu, H.; Zhang, D. Modification of the Green Fluorescent Protein Chromophore with Large Aromatic Moieties: Photophysical Study and Solid-State Emission. *Asian J. Org. Chem.* **2012**, *1*, 352-358.

35. Huang, G. J.; Ho, J. H.; Prabhakar, C.; Liu, Y. H.; Peng, S. M.; Yang, J. S. Site-Selective Hydrogen-Bonding-Induced Fluorescence Quenching of Highly Solvatofluorochromic GFP-Like Chromophores. *Org. Lett.* **2012**, *14*, 5034-5037.

36. Tsai, M. S.; Ou, C. L.; Tsai, C. J.; Huang, Y. C.; Cheng, Y. C.; Sun, S. S.; Yang, J. S. Fluorescence Enhancement of Unconstrained GFP Chromophore Analogues Based on the Push-Pull Substituent Effect. *J. Org. Chem.* **2017**, *82*, 8031-8039.

37. Ermakova, Y. G.; Sen, T.; Bogdanova, Y. A.; Smirnov, A. Y.; Baleeva, N. S.; Krylov, A. I.; Baranov, M. S. Pyridinium Analogues of Green Fluorescent Protein Chromophore: Fluorogenic Dyes with Large Solvent-Dependent Stokes Shift. *J. Phys. Chem. Lett.* **2018**, *9*, 1958-1963.

38. Deng, H.; Yu, C.; Gong, L.; Zhu, X. Self-Restricted Green Fluorescent Protein Chromophore Analogues: Dramatic Emission Enhancement and Remarkable Solvatofluorochromism. *J. Phys. Chem. Lett.* **2016**, *7*, 2935-2944.

39. Yampolsky. I. V.; Remington, S. J.; Martynov, V. I.; Potapov, V. K.; Lukyanov. S.; Lukyanov, K. A. Synthesis and Properties of the Chromophore of the asFP595 Chromoprotein from Anemonia Sulcata. *Biochemistry* **2005**, *44*, 5788-5793.

40. Deng, H.; Zhu, Q.; Wang, D.; Tu, C.; Zhu, B.; Zhu, X. GFP-Inspired Fluorescent Polymer. *Polym. Chem.* **2012**, *3*, 1975-1977.

41. Conyard, J.; Heisler, I. A.; Chan, Y.; Page, P. C. B.; Meech, S. R.; Blancafort, L. A New Twist in the Photophysics of the GFP Chromophore: A Volume-Conserving Molecular Torsion Couple. *Chem. Sci.* **2018**, *9*, 1803-1812.

42. Dong, J.; Solntsev, K. M.; Tolbert, L. M. Solvatochromism of the Green Fluorescence Protein Chromophore and Its Derivatives. *J. Am. Chem. Soc.* **2006**, *128*, 12038-12039.

43. Tou, S. L.; Huang, G. J.; Chen, P. C.; Chang, H. T.; Tsai, J. Y.; Yang, J. S. Aggregation-Induced Emission of GFP-Like Chromophores *via* Exclusion of Solvent-Solute Hydrogen Bonding. *Chem. Commun.* **2014**, *50*, 620-622.

44. Mei, J.; Leung, N. L. C.; Kwok, R. T. K.; Lam, J. W. Y.; Tang, B. Z. Aggregation-Induced Emission: Together We Shine, United We Soar! *Chem. Rev.* **2015**, *115*, 11718-11940.

45. Liang, J.; Tang, B. Z.; Liu, B. Specific Light-Up Bioprobes Based on AIEgen Conjugates. *Chem. Soc. Rev.* **2015**, *44*, 2798-2811.

46. Zhai, D.; Xu, W.; Zhang, L.; Chang, Y. T. The Role of "Disaggregation" in Optical Probe Development. *Chem. Soc. Rev.* **2014**, *43*, 2402-2411.

47. Deng, H.; Liu, B.; Yang, C.; Li, G.; Zhuang, Y.; Li, B.; Zhu, X. Multi-Color Cell Imaging under Identical Excitation Conditions with Salicylideneaniline Analogue-Based Fluorescent Nanoparticles. *RSC Adv.* **2014**, *4*, 62021-62029.

48. Adamo, C.; Jacquemin, D. The Calculations of Excited-State Properties with Time-Dependent Density Functional Theory. *Chem. Soc. Rev.* **2013**, *42*, 845-856.

49. Greenwood, J. B.; Miles, J.; Camillis, S. D.; Mulholland, P.; Zhang, L.; Parkers, M. A.; Hailes, H. C.; Fielding, H. H. Resonantly Enhanced Multiphoton Ionization Spectrum of the Neutral Green Fluorescent Protein Chromophore. *J. Phys. Chem. Lett.* **2014**, *5*, 3588-3592.

50. Epifanovsky, E.; Polyakov, I.; Grigorenko, B.; Nemukhin, A.; Krylov, A. I. Quantum Chemical Benchmark Studies of the Electronic Properties of the Green Fluorescent Protein Chromophore. 1. Electronically Excited and Ionized States of the Anionic Chromophore in the Gas Phase. *J. Chem. Theory Comput.* **2009**, *5*, 1895-1906.

51. Altoe', P.; Bernardi, F.; Garavelli, M.; Orlandi, G.; Negri, F. Solvent Effects on the Vibrational Activity and Photodynamics of the Green Fluorescent Protein Chromophore: A Quantum-Chemical Study. *J. Am. Chem. Soc.* **2005**, *127*, 3952-3963.

52. Hasegawa, J. Y.; Fujimoto, K.; Swerts, B.; Miyahara, T.; Nakatsuji, H. Excited States of GFP Chromophore and Active Site Studied by the SAC-CI Method: Effect of Protein-Environment and Mutations. *J. Comput. Chem.* **2007**, *28*, 2443-2452.

53. Polyakov, I.; Epifanovsky, E.; Grigorenko, B.; Krylov, A. I.; Nemukhin, A. Quantum Chemical Benchmark Studies of the Electronic Properties of the Green Fluorescent Protein Chromophore: 2. Cis-Trans Isomerization in Water. *J. Chem. Theory Comput.* **2009**, *5*, 1907-1914.

54. Mayer, I. Bond Order and Valence Indices: A Personal Account. *J. Comput. Chem.* **2007**, *28*, 204-221.

55. Mayer, I. Improved Definition of Bond Orders for Correlated Wave Functions. *Chem. Phys. Lett.* **2012**, *544*, 83-86.

56. Mayer, I. Covalent Bonding: The Role of Exchange Effects. *J. Phys. Chem. A* **2014**, *118*, 2543-2546.

57. Carayon, C.; Ghodbane, A.; Gibot, L.; Dumur, R.; Wang, J.; Saffon, N.; Rols, M. P.; Solntsev, K. M.; Fery-Forgues, S. Conjugates of Benzoxazole and GFP Chromophore with Aggregation-Induced Enhanced Emission: Influence of the Chain Length on the Formation of Particles and on the Dye Uptake by Living Cells. *Small* **2016**, *12*, 6602-6612.

58. Liao, C.; Li, F.; Huang, S.; Zheng, B.; Du, J.; Xiao, D. A Specific and Biocompatible Fluorescent Sensor Based on the Hybrid of GFP Chromophore and Peptide for HSA Detection. *Biosens. Bioelectron.* **2016**, *86*, 489-495.

59. Lin, C. J.; Zeininger, L.; Savagatrup, S.; Swager, T. M. Morphology-Dependent Luminescence in Complex Liquid Colloids. *J. Am. Chem. Soc.* **2019**, *141*, 3802-3806.

For Table of Content Entry Only

Dual-Self-Restricted GFP Chromophore Analogues with Significantly Enhanced Emission

Hongping Deng, Chunyang Yu, Deyue Yan,* and Xinyuan Zhu**